RUSLE-GIS/RS based prediction of soil loss from Liangzi Lake watershed, Hubei, China

Sakinatu Issaka[a], Muhammad Aqeel Ashraf[a,*], Prosper Basommi Laari[b], Gomolemo Valencia Fritz[a]

[a]*School of Environmental Studies, China University of Geosciences (Wuhan), 388 Lumo Road, Wuhan 430074, China*
[b]*Department of Environmental Resource Studies, University for Development Studies, Wa campus, Upper West Region, Ghana, email: chemaqeel@gmail.com (M.A. Ashraf)*

ABSTRACT

The revised universal soil loss equation (RUSLE) interpreted with geographic information system and remote sensing (GIS and RS) criteria were used to predict possible soil loss in the Liangzi Lake watershed. Soil erosion within the watershed was varied spatially during this study. Spatial variations of various erosion vulnerable zones within the watershed using RUSLE criteria. The absence of conservational practices led to the highest potential of soil erodibility along the bare land area which was 15.2% of the catchment area. The spatial and quantitative soil loss evidence obtained through simulation of RUSLE parameter through GIS and RS techniques in Liangzi Lake watershed is more effective compared to ground-based observations. This method can be simulated in other places for assessment and delineation of erosion-prone zones, prioritization of conservation practices, and evaluation of different land management practices. The outcomes of this study integrate spatially distributed soil loss rate and erosion risk map of Liangzi Lake watershed. The annual soil loss of the watershed ranged from about 482.63-ton ha^{-1} y^{-1} to about 488.20-ton ha^{-1} y^{-1}, with an estimated average loss of about 485.42-ton ha^{-1} y^{-1}. Furthermore, the slope length and gradient factors were the primary significant RUSLE parameter followed by the soil erodibility (K) factor.

Keywords: Soil erosion; Soil loss; Revised universal soil lost equation; Geographic information system; Remote sensing

1. Introduction

Lake shrinkage and pollution is major natural concern in the ecosystems and the greatest impacting factor is linked to soil erosion facing threats under intensified land management practices and climate change, the gradual accumulation of sediments along catchments and into water bodies eventually leads to a reduction in the shape of the area of lakes [1].

Globally, there is great concern over tracing lake changes, lake shrinkage, wetland degradation and their mediating factors to reduce the impact on ecological systems [2,3]. In East Asia, the lower reaches of the Yangtze constitute the largest cluster of freshwaters, which performs a delicate role in runoff regulation, potable water for human consumption, social development and flood control of which Liangzi Lake is inclusive [4]. This area is classified as one of the most densely populated regions which make up 30% of the total population of China. However, among anthropogenic activities like urbanization improper practices, and natural factors include climate change, flooding reduction in soil water holding capacity and water siltation [5,6]. Soil erosion or sediment accumulation is the greatest impacting natural factor in lake shrinkage. A major challenge in monitoring and evaluating the soil erosion process for sustainable development of natural resources is by

* Corresponding author.

recognizing susceptible areas and determining the yields of deposits in the fields [7].

Soil erosion is quantified using the average amount of soil eroded from the area within a specified duration. According to Issaka and Ashraf [7] and Yan et al. [8], the sediment yield and rate of soil detached, transported and deposited through surface water within a certain geological location and specific time scale, which serves as the main factors procedure in catchment erosion and used to control water quality activities.

Severe soil erosion causes excessive silt export to lakes causing deterioration of water quality and lake shrinkage. However, less information is known as to how much sedimentation has contributed to the reduction and recent changes that occurred. Therefore, the processes and interactions involved in prioritizing watershed management are essential to plan according to the changes.

Several modeling approaches are applied to estimate soil erosion rates by the water where strategies are assessed and implemented. The difference in these models is based on inputs, complexity and spatial-temporal attributes [9].

One of the largely adopted empirical models developed for measuring sheet and rill erosion is the universal soil loss equation (USLE) designed by Wischmeier and Smith [10] and the first edition of the agricultural handbook soil erosion for water modeling by Renard et al. [11] which provides references for conservation guidelines and planning, with improvement t and time, it was later revised as the revised universal soil loss equation (RUSLE).

This research proposes to demonstrate its efficiency in obtaining results by computing information and a technical geographic information system (GIS) base to map Liangzi Lake watershed and integrate with RUSLE applied with success by the study of Wischmeier and Smith [10], Sismaka et al. [12] and Okon et al. [13]. The main goal of this study is to predict the erosion rate with its associated effects on water quality deterioration in the lake system.

2. Materials and methods

2.1. Description of the study area

Liangzi Lake watershed is among the top ten lakes in china and the second freshwater lake in Hubei Province, it is also home to Wuchang breams with its popular large mitten crabs. The watershed (30°3–19′N; 114°26–38′E) is located on the southern bank of the middle reaches of the Yangtze River by 43.3 km channel (Fig. 1). The lake has an area of 227.26 km^2 in the dry season and 499.77 km^2 in the wet season, and a depth of 3–5 m and a total area of 304.3 km^2, with a drainage area of 3,265 km^2, mean width of 9.6 km and an elevation of 20 m, over 31.7 km length.

According to the Pollution and Agency, the Liangzi Lake watershed includes numerous bays or fingers which include 30 rivers flowing into it, with the biggest being the Gaoqiao River [14]. The lake system also includes Ya'er Lake, Bao'an, Niushan, and Sanshan Lakes, with an average water retention period of 193 d longer.

The subtropical continental monsoon climate in the area in winter is cool and dry, and summer is humid and warm with a mean annual rainfall of 1,330 mm, with 17°C mean average temperature. Also, the prolonged raining season makes the area susceptible to soil loss which lasts from July to November throughout the year.

2.2. Field survey and data collection

A field survey was carried out to observe the Liangzi Lake watershed landscape and geological features, soil profile slope conservation techniques and the various activities carried out around the watershed such as recreational, farming, fishing [15]. A geographical positioning system (GPS) was used to survey the sample sites and to determine the coordinates, to ensure the actual locations of these sites during subsequent sampling periods. Soil samples were obtained along with selected samplings points in the catchment (Fig. 2).

The rainfall data for 2016–2017 were gotten from the Hubei Climatology Station (www.data.cma.cn). Furthermore, spatial data analysis was obtained using GIS and remote sensing (RS) software's to determine the erosion potential and spatial distribution of the study area using the United States Geological Survey (USGS) data center. The study location was digitized using land use and topographic maps, the soil map was attained from the Chinese department of agriculture topographic and land–use maps. The soil map for this study was obtained from the Chinese agricultural department to be able to ascertain the measurement of soil erodibility factor using RUSLE.

2.3. Soil texture

Soil textural analysis was undertaken using the modified hydrometer method according to the China Standard (F-HZ-DZ-TR-0008), which depends on the soil reaction (pH) of the samples. About 50 g of soil with pH less than 7.5 but more than 6.5 were reacted with 50 mL sodium oxalate ($Na_2C_2O_4$) in an Erlenmeyer flask at a constant time of 1 h on a small heater to boil, in order to facilitate the dispersion of the soil particles. The boiled solutions were cooled and poured into a 1,000 mL volumetric cylinder. The Erlenmeyer flask was washed thoroughly with deionized water, after which the solution was increased to 1 L using deionized water, and then stirred for 5 min [16–18]. All samples were designed to have a constant soil-to-dispersant reagent ratio (1:1) from 1 min as a minimum reaction time to maximum reaction time of 8 h. Then from the hydrometer readings the percentage of grains was obtained as follows:

(1) Clay % = (Reading2 × (5 min) + Reading3 × (8 h)) ÷ (Soil weight) × 100.
(2) Silt % = ((Reading1 ÷ Soil weight) × 100) – Clay%.
(3) Sand % = 100 – Silt% – Clay%. The soil texture nomograph was used to plot the percentages ratios of clay, silt, and sand.

2.4. Mathematical modeling and statistics

The RUSLE is known globally to forecast the potential soil loss associated with erosion. For the accurate prediction model of soil loss rate, previous studies relied on the proper parameter values and data. More so, RUSLE was the
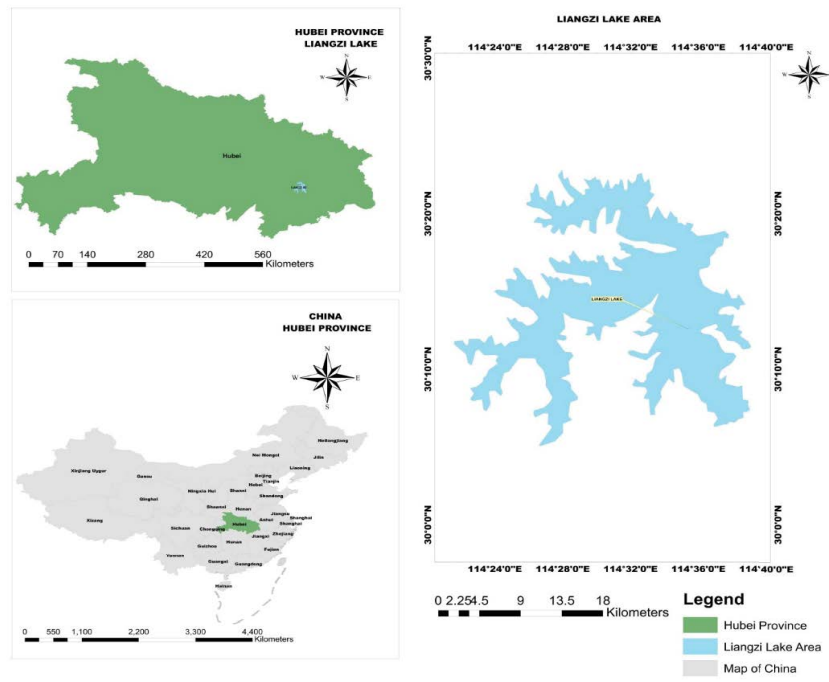
Fig. 1. Location of the study area.
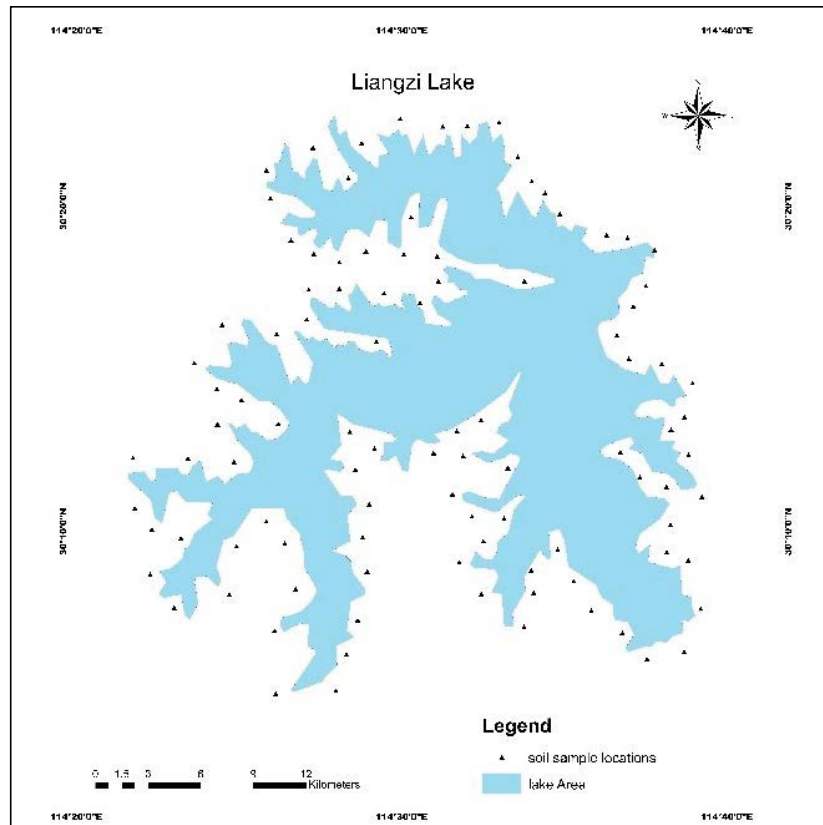
Fig. 2. Soil sample locations.

preferred model due to its available data, accurate results and easy implantation. Hence, the 2016/2017 eroded soil and sediments loads at the watershed were simulated using the RUSLE model.

To calculate the adopted formula for the RUSLE is:

$$A = R \times K \times LS \times C \times P$$

where A is the rainfall erosivity index (MJ mm ha^{-1} y^{-1}); K is the soil erodibility index (ton h MJ 1 mm^{-1}); L is the slope length factor (m); S is the slope steepness factor (%); C is the vegetation cover factor; P is the soil conservation practice factor.

The RUSLE was required to utilize some assessment for soil erosion factors. The factors used were R, K, LS and P which were utilized to calculate soil loss in the study area. The various factors mentioned above are described.

2.5. Rainfall erosivity index (R)

The rainfall erosivity index (R) is sometimes used interchangeably with the erosivity (E) index is to determine the erosion potential of precipitation expected within a specific area and raindrop impact which must reflect the quantity and rate of runoff on the soil associated with the rain. R index is largely related to the intensity of rain and kinetic energy. In this study, the calculation is based on Morgan [19] who stated that the best-estimated values for erosivity index for any area should be an average of two values because the R values can be present in any area.

The indexation for the tropical region according to Wischmeier and Smith [10] the maximum rainfall intensity recommended 75 mm h^{-1} due to the fact that raindrop size decreases when intensity exceeds the threshold value. The R represents total annual rainfall and it was calculated as follows:
R factor calculation:

Morgan: $R = (9.28P - 8,838.15) \times 75$ in metric units

Roose: $R = P \times 0.5 \times 1.73$ in metric units

where P = total annual.

2.6. Soil erodibility index (K)

Soil erodibility is the external force applied to soil to change its original formation. Hence, soil detached by splash during rainfall from a higher elevation to catchment areas by water depends on soil structure particle size composition, organic matter percentages and soil oil permeability measured as hydraulic conductivity. The K value is obtained using a nomograph [20,21], and to calculate the K value of the soil in this study area, the equation proposed by Foster et al. [22] were used:
where $K = [2.1 \times 10^4 (12-OM)M1.14 + 3.25(S-2) + 2.5(P-3)]/100$; M = the product of the primary particle size fraction (% modified silt or the 0.002–0.1 mm size fraction) × (% silt + % sand); K is the soil erodibility index in tons/ac (100 ft.-tons in/ach). Division of the right side of this equation

with 7.59 will yield K values expressed in SI units. S = soil structure code. P = soil permeability class (hydraulic conductivity) [23].

To estimate the soil erodibility or the values of the K factor in this study area, soil samples were collected and analyzed for their organic matter content, particle size distribution, hydraulic conductivity and textural classification. Based on the relative proportions of clay, silt, sand, and organic matter, the soil erodibility factor was estimated in ton h MJ^{-1} mm^{-1}.

2.7. Topographic factor (LS)

Within the RUSLE equation, the LS factor represents the effects of topography on erosion, the slope length factor (L) reflects the effect of the slope length on erosion, and the slope steepness factor (S) represents the influence of the slope gradient on erosion. The slope factor (LS) is combined with the slope gradient and the length of the eroding surface into a single factor. Under RUSLE, LS denotes the actual length of the overland flow path, and it is the distance from the source of the overland flow to a point where it enters a major flow concentration. This definition is particularly relevant for forested or vegetated watershed areas where the overland flow seldom exists on hill slop [24].

The subsurface storm flow is more prevailing than the overland flow in forested watershed areas, and the latter only exists in limited areas near the channel margins or on shallow soil as the return flow or saturated overland flow [24]. Subsequently, the overland flow path in the forested watershed is expected to be shorter than the slope length identified from the map. The slope length and gradient were calculated from the topographical map of the study area. Upon obtaining the L and S values, the topographical factor (LS) values were calculated using the formula adopted from Van Remortel et al. [28]:
The LS factor is estimated based on:

$$L = (\lambda/22.13) \text{ m};$$

$$B = (\sin\theta)/[3 \times (\sin)0.8 + 0.56];$$

$$S = 10.8 \cdot \sin\theta + 0.03\theta < 9\%;$$

$$S = 16.8 \cdot \sin\theta - 0.5\theta \geq 9\%$$

where L is the slope length (m); λ is the slope length (it is the horizontal projection, not distance parallel to the soil surface); m is the variable slope length exponent; S is the slope gradient (%).

2.8. Vegetation cover factor (C)

The vegetation cover factor (C) designates the ratio of soil loss under a given vegetation cover as opposed to that on bare soil. The C factor is used to reflect the effect of cropping and management practices on soil erosion rates in agricultural areas and the effects of the vegetation canopy and ground cover on reducing soil erosion in forested regions [25,26]. It was adopted from Table 1 in this study.

Table 1
Land cover management, *C* factor for forested and undisturbed land

Erosion control treatment	*C* factor	Erosion control treatment	*C* factor
Rangeland	0.23	Mining areas	1.00
Forest/Tree		Agricultural area	
		Agricultural crop	0.38
25% cover	0.42	Horticulture	0.25
50% cover	0.39	Cocoa	0.20
75% cover	0.36	Coconut	0.20
100% cover	0.03	Oil palm	0.20
		Rubber	0.20
Brusher/Scrub		Paddy	0.01
25% cover	0.4	Urbanized area	
50% cover	0.35	Residential	
75% cover	0.3	Low density (50% green area)	0.25
100% cover	0.03	Medium density (50% green area)	0.15
		High density (50% green area)	0.05
Grassland (100% coverage)	0.03	Commercial, education and industrial	
		Low density (50% green area)	0.25
Swamps/Mangrove	0.01	Medium density (50% green area)	0.15
		High density (50% green area)	0.05
Water body	0.01	Impervious (parking lot, road, etc.)	0.01

Modified from Shin [27]

The efficacy of a plant cover for reducing erosion depends on the height, continuity of the tree canopy, the density of the ground cover and root growth. The vegetation cover intercepts raindrops and dissipates their kinetic energy before they reach the ground surface. The relative impact of management options can be easily compared by making changes in the *C* factor, which vary from near zero for well-protected land cover to one for barren areas. The *C* factor is calculated based on:

If NDVI = 0, then $C = 0$, else, $C_i = -1.25(\text{NDVI})\, i + 1$

Also, there are some pre-determined *C* factor values that can be used in the estimation process (Table 1).

2.9. Conservation factor (P)

Contouring effect and tillage practices on soil erosion are described by the support practice factor *P* within the RUSLE model. Wischmeier and Smith [10] defined the support practice factor *P* as the ratio of soil loss with a specific support practice to the corresponding soil loss due to up and down cultivation. Table 2 shows the value of the *P* factor based on the cultivating methods and slope [27]. The *P* values range from 0 to 1, with the value 0 representing a very good man-made erosion resistance facility, whilst the value 1 represents no man-made resistance erosion facility.

The lower the *P*-value (Table 2), the more effective the conservation practice is at reducing soil erosion. If there are no support practices, the *P* factor is 1.00. Modern agricultural practices consist of up and down tillage without the presence of contours, strip cropping or terracing.

The *P* factor depends on the conservation measure applied within the study area. The most common conservation measure in China is contour terracing. The value of *P* was assigned by overlaying the slope map and land-use map.

3. Results and discussions

3.1. Evaluation of soil erosion model

3.1.1. Land use distribution of the Liangzi Lake watershed

Land use/cover of the Liangzi Lake area can be classified into 8 categories, thus, paddy fields, dry land, orchard, tea gardening, vegetable cultivation, gardening, grassland, and woodland. These are summarized into dry land, paddy and gardens, forest and orchard, and grass (Fig. 3).

3.1.2. Soil loss rate assessment

The RUSLE model was integrated into this study with GIS and RS techniques to determine the mean annual soil loss rate (t ha^{-1} y^{-1}) and to detect and map soil erosion-prone areas at the Liangzi Lake watershed. The Raster maps of the RUSLE parameters resulting from different data sources were produced and discussed as follows.

3.1.3. Rainfall erosivity (R) factor

The erosivity factor estimated by Roose's equation ranges from 573.68 (Huangshi station) to 1,325.43 (Yingshan station). The average *R*-value of Ezhou station which is quite close to the studied watershed is 1,303.6 which has a great weight to the *R*-value of the watershed (Table 3).

Table 2
P factor according to the types of cultivation and slope (modified from Shin, G.J. 1999)

Slope (%)	Contouring	Strip cropping	Terracing
0.00–7.00	0.55	0.27	0.1
7.00–11.30	0.6	0.3	0.12
11.30–17.60	0.8	0.4	0.16
17.60–26.80	0.9	0.45	0.18
26.80>	1	0.5	0.2

Modified from Shin [27]
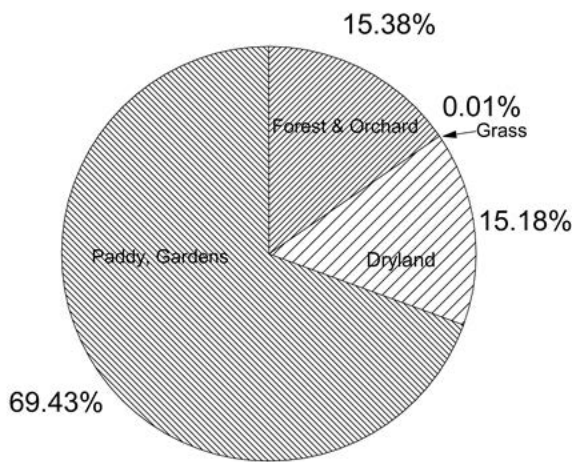
Fig. 3. Liangzi Lake watershed land use composition.

The highest average annual rainfall was recorded at Yingshan station (127.69 mm), whilst the lowest was recorded at Guangshui (48.03 mm). The estimated *R*-factor ranged from 498.56 MJ mmh⁻¹ ha⁻¹ y⁻¹ (Guangshui) to 1,325.43 MJ mmh⁻¹ ha⁻¹ y⁻¹ (Yingshan). The average estimated *R*-factor value for the selected stations was 1,011.52 ton ha⁻¹ y⁻¹ (Table 3). The rainfall factor layer was generated with ESRI ArcGIS over the whole study area, by using an inverse distance weighting interpolation algorithm on a 90 m resolution. The resultant digital elevation model is shown in Fig. 4. From the developed *R*-factor map the lowest predicted annual soil loss was 482.63 t ha⁻¹ y⁻¹, whilst the highest was 488.20 t ha⁻¹ y⁻¹ (Fig. 4).

3.1.4. Soil erodibility (K) factor

The *K*-factor values of the research study area comprise three soil classes (clay, sand and silt), with clay been the dominant soil type in the samples studied. Therefore, the *K*-factor value was assigned to each soil class with special reference to their physicochemical properties (Fig. 5).

From Fig. 4 the *K*-factor values range from 0.11 within the middle-lower section to 0.50 at grey colored portions. In between the lowest and highest are the intermediate parts marked grey, yellow and deep brown.

Table 3
Mean annual rainfall and the corresponding *R*-factor value

Station	Jingzhou	Ezhou	Huangshi	Jiayu	Macheng	Guangshui	Wuhan	Tianmen	Zhongxiang	Yingshan
Longitude	115.0325472	114.8948361	115.0388361	113.939275	114.2655361	113.8258889	114.3049694	113.1658417	112.5881222	115.6812556
Latitude	30.20523056	30.39194167	30.20003056	29.97073611	30.61379444	31.61685278	30.59236111	30.65307778	31.16782222	30.73495556
Average rainfall	81.48	125.59	55.27	127.5	102.8	48.03	119.38	103.83	82.92	127.69
R-factor [MJ mmh⁻¹ ha⁻¹ y⁻¹]	845.78	1303.6	573.68	1323.45	1067.08	498.56	1239.18	1077.74	860.71	1325.43
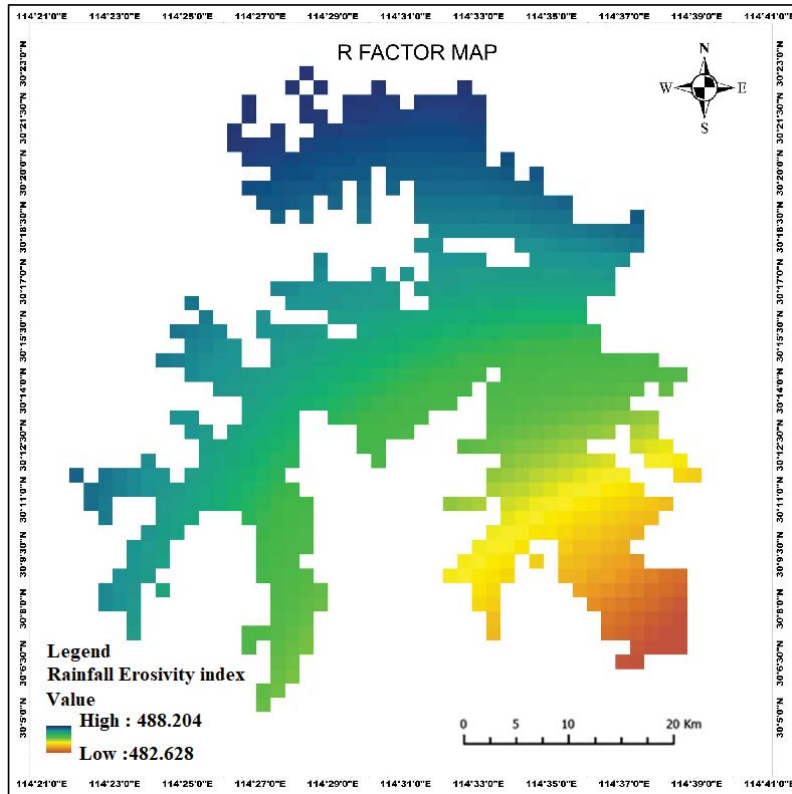
Fig. 4. Rainfall erosivity factor map.
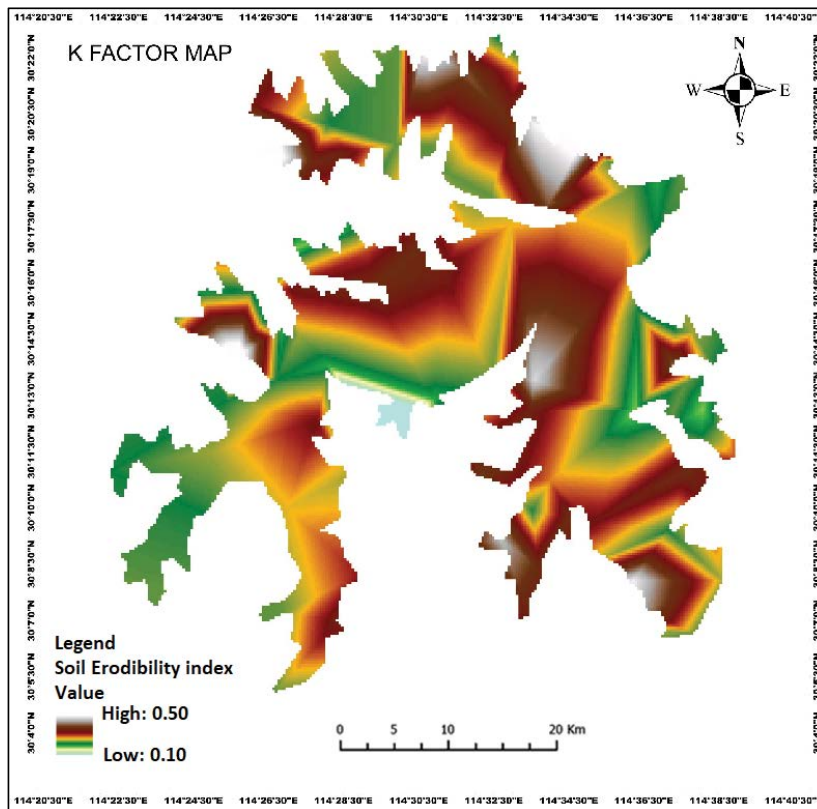
Fig. 5. Soil erodibility factor map.

3.1.5. Slope length and steepness (LS) factor

The topographic factor of RUSLE was calculated using the suggestion by Van Remortel et al. [28].

Thus, $L = (\lambda/22.13)$ m, and $LS =$ power ("Fac" × 90/22.13 – 0.4) × power (sin (slope_dem_cm1 × 0.01745)/0.09, 1.4) × 1.4.

The slope length was substituted by upslope contributing area so as to take into account the flow divergence, convergence and in a three-dimensional complex terrain condition. Hence, the contributing factor of the upstream and slope angle were all considered in the abovementioned method of slope length and gradient factor estimation. As shown in Fig. 6 (violet color), the slope length is high in the lower section of the watershed due to the high-flow accumulation (upstream contributing area), and low in the upper (light blue) and ridge part of the watershed due to the little contributing pixel upstream of the ridge.

As shown in Fig. 6, the slope length (L sub-factor) and gradient (S sub-factor) could not be independent explanatory soil loss factors. Therefore, the combined LS factor was illustrated as shown in Fig. 6. Consequently, the LS factor of RUSLE extends from 0 in the lower part of the watershed to 7655 in the steepest slope upper part of the watershed. This suggests that the effect of the combined slope length – steepness (LS) factor for soil loss is significant in the upper part of the watershed. On the other hand, the topographic (slope length – steepness) factor contributes slightly to soil erosion in the lower and middle parts of the watershed (Fig. 6).

3.1.6. Cover and management (C) factor

The major land use/covers of the watershed identified by supervised image classification were recreational, fishing, forest land, shrubland, water body, and cultivated land. Vegetables were found as a dominant crop cover in the Liangzi watershed. Most of the corresponding land cover factor was obtained from different studies [28] (Table 1).

Most of the lower catchments of the watershed are covered by cropland (vegetables), so these parts of the watershed have the highest C-factor value. This is because vegetables do not reduce the direct impact of rainfall on soil resources like forest land. Whereas most of the upper catchments of the watershed are dominated by scattered shrubland and assigned the C-value of 7. Therefore, it can be concluded that the contribution of crop and management factors for the soil erosion model is higher in the case of cultivated land (Fig. 7).

3.1.7. Erosion management (support) practice (P) factor

The P factor ranges from 0 to 1, the value closer to 0 indicates good conservation practice and the value closer to 1 indicates poor conservation practice. As explained in detail earlier, the Wischmeier and Smith [29] method of calculating the P-value was applied in this study. Therefore, areas in this study containing water, shrubs, and other vegetation were assigned as other lands given the P-value of
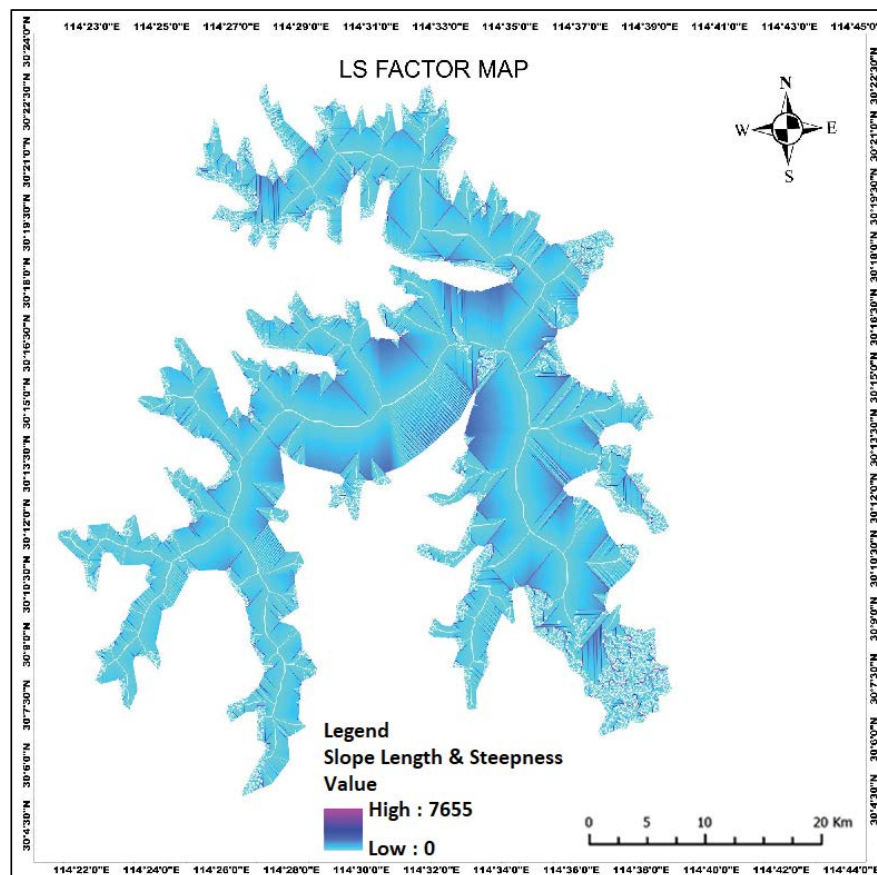
Fig. 6. Slope length and steepness factor.
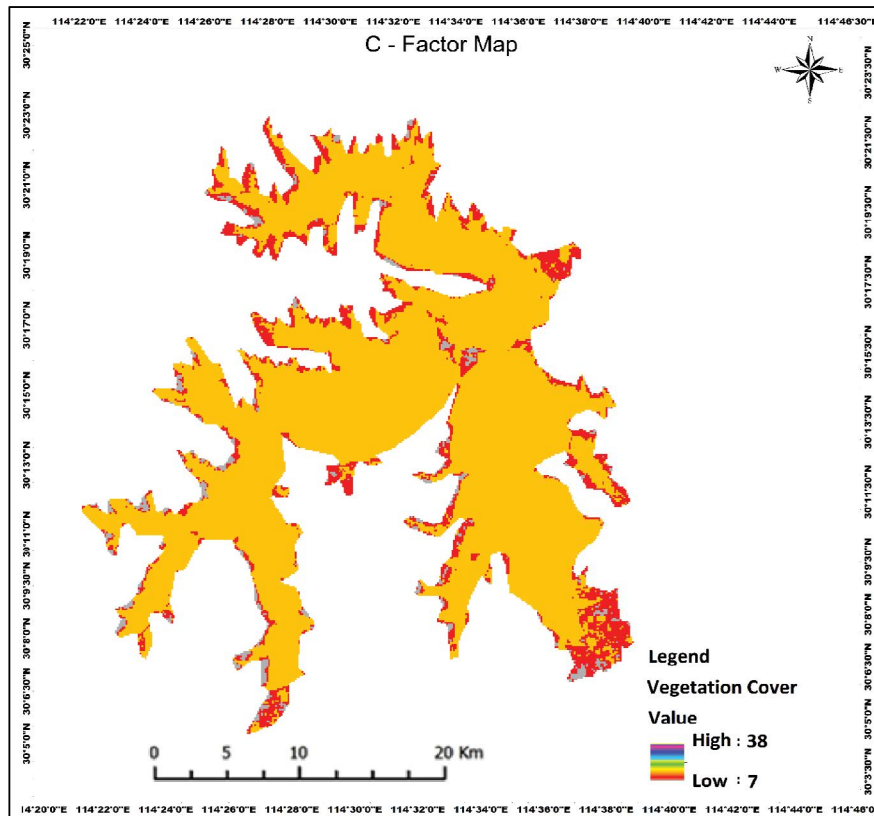
Fig. 7. Cover and management (*C*) factor.

1.00 regardless of their slope class, whereas the cultivated areas were given a different *P*-value (Fig. 8).

Finally, the thematic land use and land cover; and slope map of the watershed were transformed to vector format to assign the *P*-value, and a Raster map of the *P*-factor was created. As illustrated in Fig. 8, most of the upper catchment and some of the northeastern middle parts of the watershed exhibit a high *P*-value. On the contrary, most of the lower parts of the watershed have the lowest *P*-value of near 0.1. This implies that the upper catchments of the watershed where erosion management practices were not yet conducted, shrub and grass/grazing lands are dominant. Also, the highest slope classes are dominant and have a significant contribution to erosion.

3.1.8. Water flow measurement

The water flow rate from the lake was estimated by a current flow meter. After which the simplified form of the continuity equation was applied based on the methodology used for measurement and estimation of the water flow rate. Using an estimated length of 10 m and width of 10 m, the average daily flow rate/discharge rate of the Liangzi Lake was estimated at 385 $m^3 s^{-1}$. Compared with the study carried out by the study of Sidle and Chigira [30], therefore, implies that the flow rate of the water is gradually decreasing, as a result of siltation and a possible increase in growth of aquatic weeds or eutrophication caused by deposition of nutrients washed into the lake through erosion.

According to Xu et al. [31] the building of water conservancy facilities (e.g., sluice gates), affected sedimentation rates by controlling the outflow/inflow of sediments or changing the hydrodynamic force (due to the changes in water flow rates) for particle deposition. In contrast, Xiang et al. [32] examined 8 lakes basin in the middle reach of the Yangtze River and found that sediment accumulation rates are due to seasonal hydrological regimes of water exchange with the Yangtze River and not sediment deposition only. Therefore, if this trend continues, the volume of the lake will eventually reduce, thereby transforming the lake into a state that will reduce its water carrying capacity or change its shape.

3.1.9. Annual precipitation data for selected meteorological stations used to determine rainfall factor

The annual precipitation data covering 2016 and 2017 for 10 selected meteorological stations within Hubei Province, China (Jingzhou, Ezhou, Huangshi, Jiayu, Macheng, Guangshui, Wuhan, Tianmen, Zhongxiang, Yingshan) were selected in order to determine the rainfall factor (*R*) for the Liangzi Lake watershed area.

From Table 3 the highest annual rainfall for the selected referenced stations in 2016 was recorded by Yishang (1,747.18 mm), whilst the lowest was recorded by Huangshi (547.82 mm). Also, in 2017 the lowest annual rainfall figure was recorded by Guangshui (486.9 mm), whilst the highest was recorded by Jiayu (1428.5 mm).
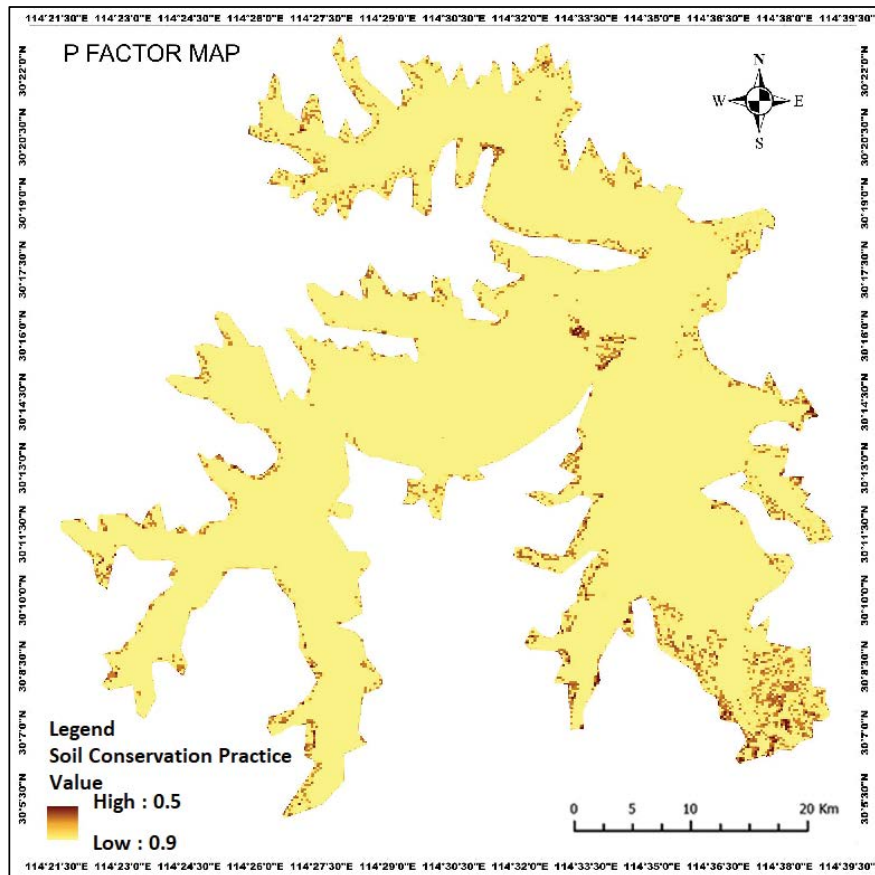
Fig. 8. Erosion management (support) practice factor map.

4. Conclusions

The RUSLE and GIS and RS methodologies were used to predict potential soil in the Liangzi water watershed. Soil erosion within the watershed varied spatially during this study. Spatial distributions of different erosion-vulnerable zones were identified within the watershed using the RUSLE criteria. The potential rate of soil loss was high in the bare land areas. In these areas, soil erosion was greater because of high soil erodibility potential and the absence of conservation practices. Anthropological activities pose the highest risk factors to the Liangzi Lake environment. Lack of proper management practices in the study area resulted in high erosion and loss of significant plant nutrients, thereby reducing the productivity of the soil, which might increase the production costs resulting from increased plant nutrient inputs as supplements. Furthermore, the losses channeled into Liangzi Lake contribute to reducing its water quality. The spatial and quantitative soil loss evidence acquired through the simulation of RUSLE parameters by GIS and RS techniques in the Liangzi Lake watershed affords the handling of spatially variable data easily and efficiently, where ground-based observation is difficult. This method can therefore be replicated in other locations for the assessment and delineation of erosion-prone zones, prioritization conservation practices, and evaluation of the usefulness of different land management practices. The outcomes of this study integrate spatially distributed soil loss rate and erosion risk map of Liangzi Lake

watershed. The annual soil loss of the watershed extends from about 482.63-ton ha^{-1} y^{-1} (lower right section of the watershed) to about 488.20-ton ha^{-1} y^{-1} at the upper left section of the watershed, with an estimated average loss of about 485.42-ton ha^{-1} y^{-1}. Therefore, the slope length and gradient (*LS*) factor was the primary significant RUSLE parameter followed by the soil erodibility (*K*) factor.

Conflict of interest

All authors declare that they do not have any conflict of interest in this study. Also, this article does not contain any studies with human participants or animals.

References

[1] J.B. Smith, H. Schellnhuber, M.M.Q. Mirza, S. Fankhauser, R. Leemans, L. Erda, L. Ogallo, B. Pittock, R. Richels, C. Rosenzweig, Vulnerability to Climate Change and Reasons for Concern: A Synthesis, J.J. McCarthy, O.F. Canziani, N.A. Leary, D.J. Dokken, K.S. White, Eds., Climate Change,

Impacts, Adaptation, and Vernerability, Cambridge University Press: Cambridge, UK, 2001, pp. 913–967.

[2] J. Wang, Eco-Services for Urban Sustainability in the Yangtze River Delta of China: Strategies for Physical Form and Planning, Ph.D. Thesis, Melbourne School of Design, Faculty of Architecture, Building and Planning, The University of Melbourne, 2012.

[3] A. Earle, A.E. Cascão, S. Hansson, A. Jägerskog, A. Swain, J. Öjendal, Transboundary Water Management and the Climate Change Debate, Routledge Taylor & Francis Group, United Kingdom, London, 2015.

[4] J. Wang, Y. Sheng, T.S.D. Tong, Monitoring decadal lake dynamics across the Yangtze Basin downstream of Three Gorges Dam, Remote Sens. Environ., 152 (2014) 251–269.

[5] R. Adrian, C.M. O'Reilly, H. Zagarese, S.B. Baines, D.O. Hessen, W. Keller, D.M. Livingstone, R. Sommaruga, D. Straile, E. Van Donk, G.A. Weyhenmeyer, M. Winder, Lakes as sentinels of climate change, Limnol. Oceanogr., 54 (2009) 2283–2297.

[6] I.C. Pope, B.K. Odhiambo, Soil erosion and sediment fluxes analysis: a watershed study of the Ni Reservoir, Spotsylvania County, VA, USA, Environ. Monit. Assess., 186 (2014) 1719–1733.

[7] S. Issaka, M.A. Ashraf, Impact of soil erosion and degradation on water quality: a review, Geol. Ecol. Landscapes, 1 (2017) 1–11.

[8] R. Yan, X. Zhang, S. Yan, H. Chen, Estimating soil erosion response to land use/cover change in a catchment of the Loess Plateau, China, Int. Soil Water Conserv. Res., 6 (2018) 13–22.

[9] P. Panagos, P. Borrelli, J. Poesen, C. Ballabio, E. Lugato, K. Meusburger, L. Montanarella, C. Alewell, The new assessment of soil loss by water erosion in Europe, Environ. Sci. Policy, 54 (2015) 438–447.

[10] W.H. Wischmeier, D.D. Smith, Predicting Rainfall-Erosion Losses from Cropland East of the Rocky Mountains: Guide for Selection of Practices for Soil and Water Conservation, U.S. Department of Agriculture, 1965, pp. 282–284.

[11] K.G. Renard, D.C. Yoder, D.T. Lightle, S.M. Dabney, Universal Soil Loss Equation and Revised Universal Soil Loss Equation, Watershed, S., & Soil, N., 2010, pp. 137–167.

[12] Y. Sismaka, B.R. Purba, I.N. Puja, M.S. Sumarniasih, Erosion prediction and conservation planning in the Bubuh Sub-Watershed, Bangli Regency, Water Conserv. Manage., 4 (2020) 95–97.

[13] E.E. Okon, J.O. Ikeh, C.J. Offodile, Near - surface characterization of sediments of the Sokoto group exposed around Wamakko area, Northwestern Nigeria: an integrated approach, Geol. Ecol. Landscapes, 5 (2021) 81–93.

[14] K.S. Rawat, S.K. Singh, S. Szilard, Comparative evaluation of models to estimate direct runoff volume from an agricultural watershed, Geol. Ecol. Landscapes, 5 (2021) 94–108.

[15] Z.A. Zainal Abidin, N. Abdul Malek, N.H. Mohd Zin, A.J.K. Chowdhury, Rare Actinomycetes from Kuantan Mangrove Forest Sediment, J. Clean WAS, 4 (2020) 79–83.

[16] M. Mandal, N.D. Chatterjee, S. Burman, Boal (Wallago Attu) Fish Abandonment in Keleghai River, West Bengal: an idea based clarification, Environ. Ecosyst. Sci., 5 (2021) 23–26.

[17] S. Rijal, A review on soil conservation practices in Nepal, Environ. Contam. Rev., 3 (2020) 21–23.

[18] S. Khalid, Khanoranga, U. Altaf, R. Shah, G. Parveen, Drinking water quality assessment of Union Council Dhamni, Poonch, Azad Jammu and Kashmir, Pakistan, using water quality index and multivariate statistical analysis, Environ. Contam. Rev., 3 (2020) 24–31.

[19] R.P.C. Morgan, Soil Erosion and Conservation, John Wiley & Sons, Blackwall Publishing, 350 Main Street, Malden, MA02148-5020, USA, 108 Cowley Road, Oxford OX4 1JF, UK, 550 Swanston Street, Carlton, Victoria 3053, Australia, 2009.

[20] M.K. Jha, R.C. Paudel, Erosion predictions by empirical models in a Mountainous Watershed in Nepal, J. Spatial Hydrol., 10 (2010) 93.

[21] W.H. Wischmeier, Predicting Rainfall Erosion Losses, USDA Agricultural Research Services Handbook, 1978, p. 537.

[22] G.R. Foster, Advances in Wind and Water Erosion Prediction, J. Soil Water Conserv., 46 (1991) 27–29.

[23] A.H. Johari, P.L. Law, S.N.L. Taib, M.Y.S. Darrien, L.K. Yong, Development of rainfall erosivity (R) in revised universal soil loss equation (RUSLE) for an equatorial region of Sarawak, Int. J. Eng. Sci., 7 (2018) 24–35.

[24] L.A. Bruijnzeel, S.P. Sampurno, Hydrology of Moist Tropical Forests and Effects of Conversion: A State of Knowledge Review, Free University Amsterdam, 1990.

[25] S.M. De Jong, Derivation of vegetative variables from a Landsat TM image for modelling soil erosion, Earth Surf. Processes Landforms, 19 (1994) 165–178.

[26] D. Boellstorff, G. Benito, Impacts of set-aside policy on the risk of soil erosion in central Spain, Agric. Ecosyst. Environ., 107 (2005) 231–243.

[27] G. Shin, The Analysis of Soil Erosion Analysis in Watershed Using GIS, Ph.D. Dissertation, Department of Civil Engineering, Gang-Won National University, Gangwon-do, South Korea, 1999.

[28] R.D. Van Remortel, R.W. Maichle, R.J. Hickey, Computing the *LS* factor for the revised universal soil loss equation through array-based slope processing of digital elevation data using a C++ executable, Comput. Geosci., 30 (2004) 1043–1053.

[29] W.H. Wischmeier, D.D. Smith, R.E. Uhland, Evaluation of factors in the soil loss equation, Agric. Eng., 39 (1958) 458–462.

[30] R.C. Sidle, M. Chigira, Landslides and debris flows strike Kyushu, Japan, Eos, Trans. Am. Geophys. Union, 85 (2004) 145–151.

[31] M. Xu, X. Dong, X. Yang, X. Chen, Q. Zhang, Q. Liu, R. Wang, M. Yao, T.A. Davidson, E. Jeppesen, Recent sedimentation rates of shallow lakes in the middle and lower reaches of the Yangtze River: patterns, controlling factors and implications for lake management, Water, 9 (2017) 617, doi: 10.3390/w9080617.

[32] L. Xiang, X. Lu, D. Higgitt, S. Wang, Recent lake sedimentation in the middle and lower Yangtze basin inferred from 137Cs and 210Pb measurements, J. Asian Earth Sci., 21 (2002) 77–86.